Template Synthesis

DOI: 10.1002/anie.200802491

PO_4^{3-}-Mediated Polyoxometalate Supercluster Assembly**

*Xikui Fang and Paul Kögerler**

While the chemistry of discrete and networked high-nuclearity metal clusters continues to evolve steadily, understanding the driving forces and underlying principles governing the aggregation processes of such clusters remains a profound challenge.[1] The imperative need for effective control over their chemical and physical properties—exploited in catalysis,[2] bioinspired chemistry,[3] and materials science[4]—has stimulated considerable interest in the development of more rational and controllable synthetic strategies.[4b,5] In this context, methods based on templating principles promise both enhanced control and greater mechanistic predictability: the nuclearity and geometry of the resulting aggregate is strongly dependent on the size, shape, charge, and the stereoelectronic and coordinative geometric preference of the template.[6]

The template effect of anions, in particular, is being increasingly studied in supramolecular organic and coordination-chemistry systems because of its relevance to many chemical and biological processes.[7] While such templated systems may be constructed utilizing noncovalent forces ranging from van der Waals and hydrogen bonding to stronger metal–ligand coordinative interactions, kinetic (template can be removed) and thermodynamic (template becomes integral part of the product) templating phenomena can be differentiated.[8] The latter predominates anion templation in the field of polyoxometalate (POM) chemistry. For example, various anions are enclosed within the central cavities of discrete polyoxovanadates to form templated host–guest complexes of striking structural complementarity.[9] Furthermore, the structure-directing role of anionic species in the condensation of polyoxothiometalate rings was illustrated by Sécheresse and co-workers.[10] The same group also reported the construction of a copper-based polyoxotungstate cluster using halide templation.[11]

Herein, we describe the formation of a large heterochiral POM architecture, $[\{\alpha\text{-}P_2W_{15}O_{56}\}_6\{Ce_3Mn_2(\mu_3\text{-}O)_4(\mu_2\text{-}OH)_2\}_3(\mu_2\text{-}OH)_2(H_2O)_2(PO_4)]^{47-}$ (**1**), from multiple molecular components based on the trivacant derivative of the Dawson polyoxotungstate $[\alpha\text{-}P_2W_{18}O_{62}]^{6-}$. Remarkably, the construction of such a highly negatively charged, aggregated POM is mediated by a far smaller anion, phosphate. The complex, isolated as $K_{36}Na_{11}\mathbf{1}\cdot 106\,H_2O$, was prepared in the course of our efforts to modify the magnetic properties of preformed metal carboxylate clusters by introducing polyoxoanions through ligand competition. We have recently demonstrated that organic bridging ligands on a manganese carboxylate cluster may be partially replaced by polyoxoanions without altering the connectivity of the magnetic cluster core.[12] We now extend this strategy and show that complete ligand substitution can be achieved, thereby giving rise to an all-inorganic magnetic cluster based on supporting polyanion ligands. More importantly, an unexpected templating event subsequently organizes these preconceived building blocks into a supercluster, that is, a "cluster of clusters".

Synthesis of **1** is based on a heterometallic high-oxidation-state precursor **2** (Scheme 1) recently reported by Christou and co-workers.[13] The central $[Ce^{IV}_3Mn^{IV}_2(\mu_3\text{-}O)_6]^{8+}$ core of **2**

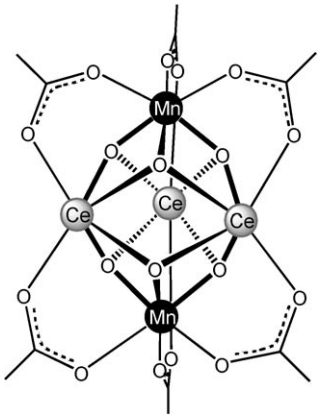

Scheme 1. Simplified core structure of the pentanuclear precursor $[Ce^{IV}_3Mn^{IV}_2O_6(O_2CMe)_{7.5}(NO_3)_3]\cdot(HO_2CMe)_{0.5}(H_2O)_2$ (**2**). For clarity, only the bridging acetate groups are shown; chelating nitrate and terminal aqua and acetate ligands are omitted.

forms a Ce_3Mn_2 trigonal bipyramid with idealized D_{3h} symmetry. Each of the six Ce–Mn edges is bridged by a μ_2-acetate ligand. The compound $K_{36}Na_{11}\mathbf{1}\cdot 106\,H_2O$ was originally obtained in very low yields (less than 0.1%) by reacting **2** with the Dawson polyoxotungstate ligand $[\alpha\text{-}P_2W_{15}O_{56}]^{12-}$. After a few weeks, only a handful of red crystals could be isolated that were suitable for X-ray diffraction analysis.[14] Examination of the molecular structure also revealed reasons for the low yields.

Crystal structure determination shows anion **1** to be a hexa-Dawson complex with crystallographic C_2 symmetry (Figure 1). The structure is best described by breaking it down

[*] Dr. X. Fang, Prof. Dr. P. Kögerler
Ames Laboratory, Iowa State University, Ames, Iowa 50011 (USA)
E-mail: kogerler@ameslab.gov
Prof. Dr. P. Kögerler
Institute of Inorganic Chemistry, RWTH Aachen University
52074 Aachen (Germany)
E-mail: paul.koegerler@ac.rwth-aachen.de

[**] We are grateful to Gordon Miller for allowing us access to X-ray facilities. Ames Laboratory is operated for the U.S. Department of Energy by Iowa State University under Contract No. DE-AC02-07CH11358.

Supporting information for this article is available on the WWW under http://dx.doi.org/10.1002/anie.200802491.

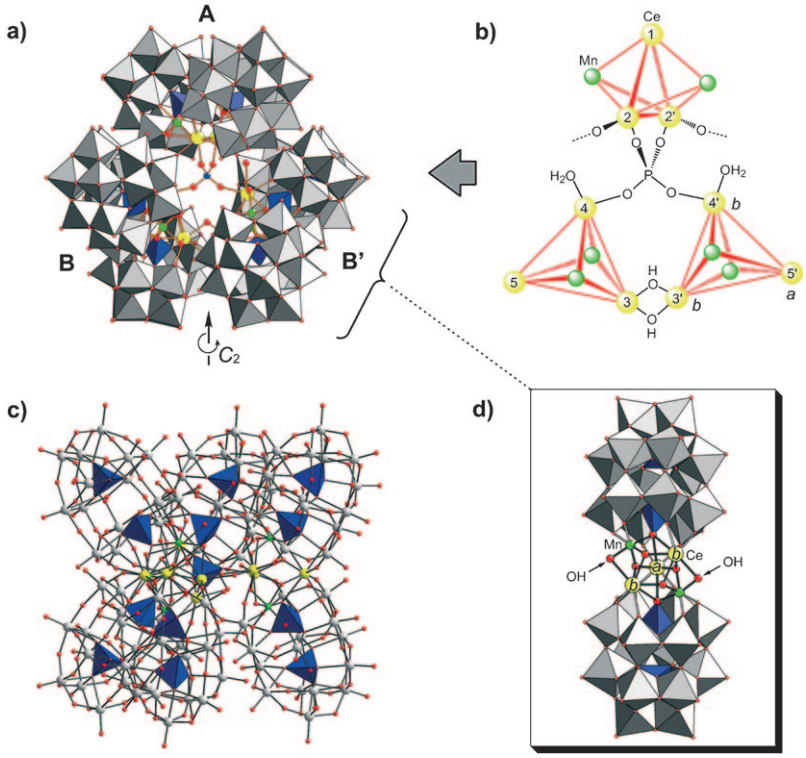

Figure 1. Structural aspects of the polyanion **1**. a) Top view showing the central templating phosphate group enclosed by three interlinked pseudo-dimers (A, B, and B′). The phosphate unit resides on a crystallographically imposed C_2 axis (relating B and B′). Color code: W gray, Mn green, Ce yellow, P blue, O red. b) Connectivity between $\{Ce^{IV}_3Mn^{IV}_2\}$ subcores and the central phosphate unit, perspective as in (a). c) A side view of the complex anion in ball-and-stick representation, with all PO_4 units highlighted as blue tetrahedra. d) Detailed structure of one Dawson dimer building block; the two types of Ce sites are designated as *a* and *b*.

into its concentric structural motifs that comprise ten primary components: six trivacant $[\alpha\text{-}P_2W_{15}O_{56}]^{12-}$ Dawson anions, three $[Ce_3Mn_2O_6(OH)_2]^{6+}$ subcore units, and a central PO_4^{3-} group.

The presence of an incorporated central phosphate anion in **1** is surprising, as no free phosphate was used initially. Yet all structural parameters unambiguously established an encapsulated PO_4^{3-} group. Phosphate impurities present in the crude starting material $Na_{12}[P_2W_{15}O_{56}]\cdot 18H_2O$ were identified as a possible source.[15] In situ generation of PO_4^{3-} from self-decomposition of $[P_2W_{15}O_{56}]^{12-}$, on the other hand, is unlikely under the present reaction conditions, explaining the extremely low yield. Indeed, in an improved synthesis in which phosphate was intentionally added, the overall yield of **1** increased to 20% (see the Experimental Section).

Even more surprising is the remarkable structural role played by the single phosphate anion in the aggregated structure. The central PO_4^{3-} fragment directs the arrangement of the giant POM framework of **1**, more than 30 Å in diameter. Overall, the complex anion may be considered as a phosphate-encapsulating macrocycle (Figure 1a) formed by three interlinked Dawson-pseudo-dimers (A, B, and B′). The three dimers resemble tilted propeller blades, thus minimizing steric repulsion arising from ligation of the central PO_4^{3-}.

Within each pseudo-dimer (Figure 1d), a $\{Ce^{IV}_3Mn^{IV}_2\}$ cluster core is encapsulated between two Dawson units, forming a sandwiched structure. Although the original pentanuclear $\{Ce_3Mn_2\}$ core of **2** is sustained in this dimeric unit, its peripheral acetate ligands have been fully substituted upon coordination with the Dawson anions. Each Dawson unit caps a Ce_2Mn triangular face and formally replaces two acetate groups bridging the corresponding Ce–Mn pairs. Moreover, a μ_2-OH[16] group is introduced on either side, substituting the two remaining acetate bridges. The ligand exchange is accompanied by significant distortion of the core geometry to meet the coordination requirements and geometric constraints of the Dawson ligands. Mn···Mn separation in the $\{Ce_3Mn_2\}$ core increases from 4.78 Å in **2** to 4.94 Å in **1** as a result; Ce···Ce and Ce···Mn distances differ significantly as well.[17]

The three Ce^{IV} centers of each dimer are in two different environments (Figure 1d). The Ce site designated as *a* directly connects the two Dawson units and is eight-coordinate (and coordinatively saturated). However, the coordination sphere of the two remaining nine-coordinate Ce centers designated as *b* are not saturated by the substituting polyanion ligands; each *b*-Ce site binds to two additional oxygen donors. In **1**, all three *a*-Ce sites (Ce1, Ce5, and Ce5′) are located on the exterior of the assembly, while the six unsaturated *b*-Ce sites (Ce2, Ce3, Ce4, Ce2′, Ce3′, and Ce4′) are directed towards the central cavity (Figure 1b). The unsaturated *b*-Ce centers represent a critical structural feature that allows cluster aggregation to occur. These sites are not only responsible for ligation to the central phosphate unit but also for interdimer bridging. First, the templating μ_4-PO_4^{3-} group holds together the three dimers by tetrahedral coordination to four *b*-Ce centers (Ce2, Ce2′, Ce4, and Ce4′): two from dimer A and one each from B and B′ (Ce–O av 2.247 Å). Furthermore, each dimeric unit is connected through *b*-Ce binding sites to its neighboring units. Dimer A is linked to the other two dimers by Ce–O=W bridges (Ce–O 2.515 Å) originating from Ce2 and Ce2′. The two symmetry-equivalent dimers, B and B′, are connected by a pair of μ_2-OH groups between Ce3 and Ce3′ (Ce–O av 2.364 Å).

An additional interesting feature of the aggregated structure of **1** is its chirality. Unlike the D_{3h} $\{Ce_3Mn_2\}$ core of **2**, each dimeric unit in **1** exhibits virtual C_2 symmetry owing to the distortion associated with ligand exchange; the twofold axis runs through the *a*-Ce center and bisects the two *b*-Ce centers (Figure 1d). The reduced symmetry enables two possible enantiomeric forms Λ and Δ[18] for individual dimeric building blocks. Interestingly, the three dimers in a given molecule of **1** are not of the same conformation, thus rendering **1** a rare heterochiral POM species; the aggregated

structure features either a ($\Lambda\Delta\Delta$) or ($\Delta\Lambda\Lambda$) ensemble, with dimer A being the enantiomeric counterpart of B and B′. Overall, the complex crystallizes as a racemic mixture in the centrosymmetric space group *C*2/*c*.

Although the three dimers are different with respect to local symmetry and chirality, their structural parameters are almost identical, implying that the dimeric unit is formed as a reaction intermediate. Accordingly, formation of the hexameric complex possibly occurs in a stepwise manner. First, ligand metathesis of **2** with polyoxoanions leads to sandwich dimers. In this initial state, coordination vacancies of each *b*-Ce site are presumably occupied by two solvent water molecules. This assumption is reinforced by the presence of residual aqua ligands on Ce4 and Ce4′ in the crystal structure of **1**. Owing to the labile nature of H_2O–Ce bonds, some of the aqua ligands are then replaced by the strongly coordinating PO_4^{3-} group, thus promoting aggregation of the dimer building blocks. In the final stage, the aggregated structure is further supported by a number of interdimer bridges after removal or deprotonation of the remaining aqua groups on the Ce centers. Furthermore, strong intramolecular hydrogen-bonding interactions also stabilize the assembly (see Supporting Information).

On the basis of magnetic susceptibility measurements (2.0–290 K, 0.1 Tesla), the cluster aggregate **1** can be described as three independent, antiferromagnetically coupled Mn^{IV} ($S = 3/2$) dimers with an overall singlet ground state. Though the geometries of the $\{Ce_3Mn_2\}$ cores of dimers A and B differ slightly, a simple model based on three identical Mn–Mn coupling interactions adequately describes the observed data. A corresponding isotropic Heisenberg model $\boldsymbol{H} = -2J\mathbf{S}_1\mathbf{S}_2$ yields a near-perfect fit to the experimental data (Figure 2) for $J = -5.1\ cm^{-1}$ and $g_{iso} = 1.98$. Note that this exchange energy is significantly higher than that reported for **2** ($-0.4\ cm^{-1}$)[13] despite longer Mn···Mn distances (4.94 vs. 4.78 Å). This difference might be due to 1) the distortion of the $\{Ce_3Mn_2\}$ core in **1** resulting in smaller Mn-O-Ce bond angles closer to 90° and 2) the presence of two additional μ_2-hydroxo groups at each $\{Ce_3Mn_2\}$ core that expand the superexchange network.

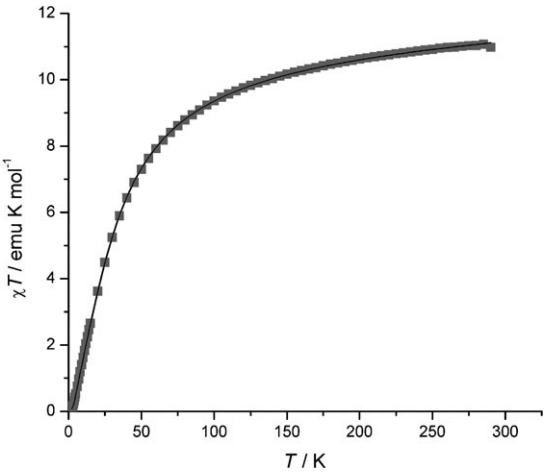

Figure 2. Temperature dependence of χT for $K_{36}Na_{11}\mathbf{1}\cdot 106\,H_2O$ at 0.1 Tesla (experimental data: gray squares; best fit to isotropic Heisenberg model: black graph).

Studies in aqueous solution suggest that the aggregated complex, once formed, is stable in solution. It does not dissociate into or equilibrate with the dimeric form to release the phosphate template. Addition of $CaCl_2$ yields no precipitation of $Ca_3(PO_4)_2$. Neither can the phosphate group of **1** in solution be displaced by other tetrahedral oxoanions such as SO_4^{2-} or ClO_4^-. As expected, the presence of multiple paramagnetic Mn^{IV} centers in **1** strongly affects the relaxation of nearby phosphorus nuclei. Solution ^{31}P NMR spectroscopy shows only a single broadened peak at $\delta = -13.9$ ppm ($\Delta\nu_{1/2} =$ 89.1 Hz), which is ascribed to well-shielded distal phosphorous atoms in the Dawson units and comparable to that measured for a related Mn^{IV} POM species.[12] The signals for the central and proximal phosphorous atoms are too broad to be observed, owing to their proximity to the Mn^{IV} centers (Figure 1c). The fact that all six distal phosphorous atoms become equivalent on the NMR timescale is attributed to their similar environments and to some degree of flexibility for the macrocycle in solution. No free phosphate signal was detected in the ^{31}P NMR spectrum.

This study demonstrates, and further confirms, that ligand metathesis constitutes a versatile tool to create novel molecule-based magnetic materials along the borderline between polyoxometalate and metal carboxylate clusters. The assembly of **1** may be considered as a good example for template-directed cluster formation. The results underline the importance of coordinatively unsaturated ("coordination number residuum") or labile binding sites, a prerequisite for further cluster aggregation. In addition, the use of template agents could be key for the buildup of increasingly sophisticated POM oligomers or aggregates. In view of this potential, the role of small inorganic anions will have to be discussed as being more important than previously thought.

Experimental Section

1: A sample of solid $Na_{12}[P_2W_{15}O_{56}]\cdot 18\,H_2O$[19] (1.16 g, 0.27 mmol) was added to a solution of **2** (0.2 g, 0.13 mmol) in H_2O (40 mL). The resulting suspension was vigorously stirred for a few minutes, and a clear solution was formed. Aqueous NaH_2PO_4 (0.1M, 0.4 mL) was then added, and the mixture was stirred for 1 h. Then, solid KCl (0.28 g, 3.8 mmol) was added and the solution heated at 80 °C for 10 min. Slow evaporation of the solution produced prismatic red crystals after two weeks (yield 0.25 g, 20% based on W). Without the addition of NaH_2PO_4, only a small amount of crystals formed and the yield was less than 0.1%. Elemental analysis (%) calcd: H 0.8, Na 0.9, P 1.4, K 5.0, Mn 1.2, Ce 4.5, W 59.3; found: H 0.9, Na 0.9, P 1.4, K 5.3, Mn 1.3, Ce 4.6, W 61.3%. IR (KBr, 1400–500 cm^{-1}): $\tilde{\nu} = 1088$(s), 1059(m), 1015(sh), 941(s), 913(s), 878(sh), 820(s), 743(s, br), 524(m), 453(w), 416 cm^{-1}(w).

Received: May 28, 2008
Published online: September 18, 2008

Keywords: cerium · manganese · phosphate · polyoxometalates · template synthesis

[1] *Comprehensive Coordination Chemistry II*, *Vol. 7* (Eds.: J. A. McCleverty, T. J. Meyer), Elsevier, Oxford, **2004**.

[2] a) M. E. Davis, *Nature* **2002**, *417*, 813; b) P.-G. Lassahn, V. Lozan, G. A. Timco, P. Christian, C. Janiak, R. E. P. Winpenny, *J. Catal.* **2004**, *222*, 260.

[3] a) V. K. Yachandra, K. Sauer, M. P. Klein, *Chem. Rev.* **1996**, *96*, 2927; b) R. Manchanda, G. W. Brudvig, R. H. Crabtreee, *Coord. Chem. Rev.* **1995**, *144*, 1.

[4] a) M. W. Cooke, G. S. Hanan, *Chem. Soc. Rev.* **2007**, *36*, 1466; b) D. Gatteschi, R. Sessoli, J. Villain, *Molecular Nanomagnets*, Oxford University Press, New York, **2006**.

[5] R. E. P. Winpenny, *Adv. Inorg. Chem.* **2001**, *52*, 1.

[6] a) R. W. Saalfrank, I. Bernt, E. Uller, F. Hampel, *Angew. Chem.* **1997**, *109*, 2596; *Angew. Chem. Int. Ed. Engl.* **1997**, *36*, 2482; b) B. Hasenknopf, J.-M. Lehn, N. Boumediene, A. Dupont-Gervais, A. Van Dorsselaer, B. Kneisel, D. Fenske, *J. Am. Chem. Soc.* **1997**, *119*, 10956; c) J. S. Fleming, K. L. V. Mann, C.-A. Carraz, E. Psillakis, J. C. Jefferey, J. A. McCleverty, M. D. Ward, *Angew. Chem.* **1998**, *110*, 1315; *Angew. Chem. Int. Ed.* **1998**, *37*, 1279; d) R. Wang, Z. Zheng, T. Jin, R. J. Staples, *Angew. Chem.* **1999**, *111*, 1929; *Angew. Chem. Int. Ed.* **1999**, *38*, 1813; e) X. Lin, D. M. J. Doble, A. J. Blake, A. Harrison, C. Wilson, M. Schröder, *J. Am. Chem. Soc.* **2003**, *125*, 9476; f) A. J. Tasiopoulos, W. Wernsdorfer, B. Moulton, M. J. Zaworotko, G. Christou, *J. Am. Chem. Soc.* **2003**, *125*, 15274; g) G. J. T. Cooper, G. N. Newton, P. Kögerler, D.-L. Long, L. Engelhardt, M. Luban, L. Cronin, *Angew. Chem.* **2007**, *119*, 1362; *Angew. Chem. Int. Ed. Engl.* **2007**, *46*, 1340.

[7] a) P. D. Beer, P. A. Gale, *Angew. Chem.* **2001**, *113*, 502; *Angew. Chem. Int. Ed.* **2001**, *40*, 486; b) R. Vilar, *Angew. Chem.* **2003**, *115*, 1498; *Angew. Chem. Int. Ed.* **2003**, *42*, 1460.

[8] a) D. H. Busch, A. L. Vance, A. G. Kolchinski in *Comprehensive Supramolecular Chemistry*, *Vol. 9* (Eds.: J.-P. Sauvage, M. W. Hosseini), Pergamon, New York, **1996**, pp. 1–42; b) G. Seeber, B. E. F. Tiedemann, K. N. Raymond, *Top. Curr. Chem.* **2006**, *265*, 147.

[9] A. Müller, H. Reuter, S. Dillinger, *Angew. Chem.* **1995**, *107*, 2505; *Angew. Chem. Int. Ed. Engl.* **1995**, *34*, 2328.

[10] E. Cadot, F. Sécheresse, *Chem. Commun.* **2003**, 2189, and references therein.

[11] P. Mialane, A. Dolbecq, J. Marrot, E. Rivière, F, Sécheresse, *Angew. Chem.* **2003**, *115*, 3647; *Angew. Chem. Int. Ed.* **2003**, *42*, 3523.

[12] X. Fang, P. Kögerler, *Chem. Commun.* **2008**, 3396.

[13] a) A. J. Tasiopoulos, T. A. O'Brien, K. A. Abboud, G. Christou, *Angew. Chem.* **2004**, *116*, 349; *Angew. Chem. Int. Ed.* **2004**, *43*, 345; b) A. J. Tasiopoulos, P. L. Milligan, Jr., K. A. Abboud, T. A. O'Brien, G. Christou, *Inorg. Chem.* **2007**, *46*, 9678.

[14] X-ray crystal analysis data for $K_{36}Na_{11}$**1**$\cdot 106H_2O$: $H_{224}Ce_9K_{36}Mn_6Na_{11}O_{468}P_{13}W_{90}$, $T = 173(2)$ K, $M = 27914.11\ g\,mol^{-1}$, monoclinic, space group $C2/c$, $a = 23.516(4)$, $b = 41.631(7)$, $c = 44.508(8)$ Å, $V = 43166(13)$ Å^3, $Z = 4$, $\mu(Mo_{K\alpha}) = 25.499\ mm^{-1}$, 135264 reflections measured, 31135 unique ($R_{int} = 0.1141$). Max/min residual electron densities: $5.53/-3.79\ e\,Å^{-3}$. The refinement converged to $R(F_o) = 0.0782$, $wR(F_o^2) = 0.1721$, and GOF = 1.088 with $I > 2\sigma(I)$. Further details on the crystal structure investigations may be obtained from the Fachinformationszentrum Karlsruhe, 76344 Eggenstein-Leopoldshafen, Germany (fax: (+49) 7247-808-666; e-mail: crysdata@fiz-karlsruhe.de), on quoting the depository number CSD-419470.

[15] a) The purity of polyoxotungstate starting material $Na_{12}[\alpha\text{-}P_2W_{15}O_{56}]\cdot 18H_2O$ is only ca. 90%, but the exact identity and composition of impurity phases remain unknown. See B. J. Hornstein, R. G. Finke, *Inorg. Chem.* **2002**, *41*, 2720; b) we have carried out the following simple tests and determined that phosphate is indeed a constituent of the impurity present. Addition of crude $Na_{12}[\alpha\text{-}P_2W_{15}O_{56}]\cdot 18H_2O$ to a dilute solution of $CaCl_2$ instantly leads to precipitation of $Ca_3(PO_4)_2$. In marked contrast, addition of the pure monovacant derivative $K_{10}[\alpha_2\text{-}P_2W_{17}O_{61}]\cdot 20H_2O$ does not cause such precipitation, and solutions remain clear for weeks. The results also indicate that the lacunary phosphotungstate ligands themselves are not likely to be the source of the free PO_4^{3-} anion.

[16] Bond valence sum calculations have been used to determine the protonation states (oxo, OH, or OH_2) of oxygen sites and the oxidation states of Ce and Mn centers in **1**. See the Supporting Information.

[17] See the Supporting Information for detailed structural comparison of the $\{Ce_3Mn_2\}$ cores in **2** and **1**.

[18] Chirality descriptors of the dimeric building blocks in **1** are formulated following the IUPAC convention for tris-chelate complexes, in which the enantiomers are distinguished using prefixes Λ and Δ. By analogy, viewed down the principle two-fold axes, the pseudo-dimers with left-handed (counterclockwise) and right-handed (clockwise)screw of the two polyoxoanion ligands are labeled with Λ and Δ, respectively. See the Supporting Information for examples.

[19] R. Contant, *Inorg. Synth.* **1990**, *27*, 106.

